

# Wet chemical synthesis and physical characterization of doped CeO<sub>2</sub> nanoparticles

J. Jasmine Ketzial, A. Samson Nesaraj\*

Department of Chemistry, School of Science & Humanities, Karunya University, (Karunya Institute of Technology and Sciences), Coimbatore (641 114), Tamil Nadu, India

---

## Abstract

Solid electrolytes based on doped cerium oxide, Ce(M)O<sub>2</sub>- $\delta$  (M = rare-earth cations), are of considerable interest for potential use in low temperature solid oxide fuel cells (LTSOFCs) due to its higher ionic conductivity than YSZ based solid electrolyte. In this research work, crystalline, pure Ce<sub>1-x</sub>M<sub>x</sub>O<sub>2</sub>- $\delta$  (where M = Gd or Sm, x = 0.10 or 0.20) based nanoparticles were prepared by chemical precipitation method in presence of surfactant (polyvinyl pyrrolidone). The intermediate compound (mixture of hydroxides) was subjected to TGA/DTA in order to find out the temperature at which the pure phase product is formed. Then, the as prepared materials were heat treated systematically at 300, 450 and 600o C for 2 h each to get phase pure materials. The resultant nanoparticles were subjected to physical characterization techniques such as, XRD, FTIR, particle size analysis and SEM. XRD results confirmed that all the powders had single-phase fluorite structure. Characteristic vibration mode of CeO<sub>2</sub> was proved by FTIR. The presence of nanoparticles (50 – 100 nm) in the prepared materials was found out by particle size measurements and SEM. The results of physical characterization of the above materials are found to be good for application as alternate electrolytes in SOFC. However, these materials can be considered as suitable alternate electrolytes in LTSOFC systems only after studying their electrical characteristics.

*Keywords:* Gd/Sm doped CeO<sub>2</sub> nanoparticles; alternate electrolytes for SOFC; chemical precipitation method; characterization

© 2014 Published by Journal of Nanoanalysis.

---

## 1. Introduction

Solid electrolytes based on doped cerium oxide (M<sub>2</sub>O<sub>3</sub> doped CeO<sub>2</sub>; where M = rare-earth or alkaline earth cations), are of considerable interest for potential use in solid oxide fuel cells (SOFCs) due to their higher ionic conductivity with respect to stabilized zirconia and a lower cost in comparison with lanthanum gallate – based phases[1-4]. Steele has found that the doped ceria electrolyte would have an ionic transference number in excess of 0.9 under realistic SOFC anodic conditions at 500 °C[5]. In addition,

---

\* Corresponding Author: E-mail address: [drsamson@karunya.edu](mailto:drsamson@karunya.edu), Phone: +091-422-2614300 Extn. 4001; fax: +091-422-2615615

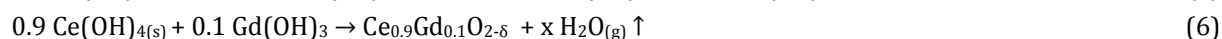
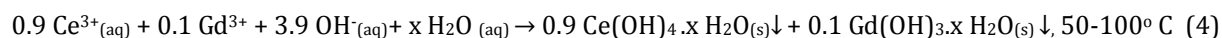
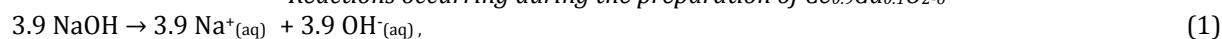
Doshi has demonstrated that doped ceria is an ionic conductor when a ceria-based SOFC is operated under load at high current density even at 600 °C, and that the electronic conduction causes leakage current only when the cell is operated at low current density at temperature above 773 K[6]. Therefore, it is widely accepted that ceria electrolytes can be employed as electrolytes in low temperature solid oxide fuel cells (LTSOFCs) operating in the range 500 – 800 °C without reduction in cell efficiency[7-9]. This advantage makes the fuel cell using ceria-based electrolyte competitive with other types of fuel cells operating at lower temperature [10,11]. Among the various dopants studied, Gd<sup>3+</sup> and Sm<sup>3+</sup> singly doped ceria (abbreviated as CGO and CSO) have been reported to have the highest conductivity [12,13]. The optimal compositions of CGO and CSO, giving the highest conductivities, were Ce<sub>0.9</sub>Gd<sub>0.1</sub>O<sub>2-δ</sub> and Ce<sub>0.8</sub>Sm<sub>0.2</sub>O<sub>2-δ</sub>[14]. Hence, the objective of this present investigation is considered as the synthesis and characterization of Ce<sub>0.9</sub>Gd<sub>0.1</sub>O<sub>2-δ</sub> and Ce<sub>0.8</sub>Sm<sub>0.2</sub>O<sub>2-δ</sub> nanoparticles by the chemical precipitation process using nitrate salts with the precipitant (sodium hydroxide) in presence of a surfactant of PVP [polyvinyl pyrrolidone]. It was reported that PVP can be used as an effective surfactant for the synthesis of nanomaterials [15]. The prepared materials were systematically characterized by suitable techniques and the results obtained were discussed and reported.

## 2. Experimental

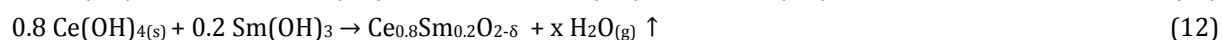
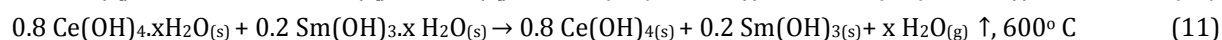
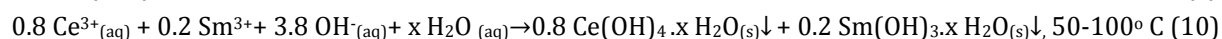
### 2.1. Preparation of Ce<sub>0.9</sub>Gd<sub>0.1</sub>O<sub>2-δ</sub> / Ce<sub>0.8</sub>Sm<sub>0.2</sub>O<sub>2-δ</sub> nanoparticles by the chemical precipitation

High purity Ce(NO<sub>3</sub>)<sub>3</sub>.6H<sub>2</sub>O, Gd<sub>2</sub>O<sub>3</sub> / Sm<sub>2</sub>O<sub>3</sub>, nitric acid, sodium hydroxide and poly vinyl pyrrolidone were used in the preparation of Ce<sub>0.9</sub>Gd<sub>0.1</sub>O<sub>2-δ</sub> and Ce<sub>0.8</sub>Sm<sub>0.2</sub>O<sub>2-δ</sub> nanoparticles. Initially, appropriate concentrations of 100 ml Ce(NO<sub>3</sub>)<sub>3</sub>, 100 ml Gd(NO<sub>3</sub>)<sub>3</sub> or Sm (NO<sub>3</sub>)<sub>3</sub> and 100 ml sodium hydroxide solutions were prepared in pure distilled water. 2 ml of 10 % PVP (surfactant) was added slowly to the sodium hydroxide solution. To this mixture, Ce(NO<sub>3</sub>)<sub>3</sub> and Gd(NO<sub>3</sub>)<sub>3</sub> or Sm (NO<sub>3</sub>)<sub>3</sub> solutions were added consequently drop wise. They were mixed by a magnetic stirring apparatus (at 1000 rpm) in room temperature for 1 hour. Throughout the experiment the pH was maintained as greater than 9 by the addition of alkali (NaOH pellets). The resultant yellow coloured precipitate [Ce(OH)<sub>4</sub> + Gd(OH)<sub>3</sub> or Sm(OH)<sub>3</sub>] was filtered, and then washed with deionized water and ethanol for about 5 – 10 times. The precipitate was dried at 50 – 100° C for 24 hours. Then, the calcination was carried out at 300, 450 and 600° C for 2 hours each. During calcination at high temperature, the surfactant was removed and phase pure yellow coloured Ce<sub>0.9</sub>Gd<sub>0.1</sub>O<sub>2-δ</sub> or Ce<sub>0.8</sub>Sm<sub>0.2</sub>O<sub>2-δ</sub> nanomaterials were formed. Figure 1 shows the schematic illustration of the synthesis of Ce<sub>0.9</sub>Gd<sub>0.1</sub>O<sub>2-δ</sub> or Ce<sub>0.8</sub>Sm<sub>0.2</sub>O<sub>2-δ</sub> by the chemical precipitation process. Main reactions which can occur during the experimental procedure can be written briefly as follows:

#### *Reactions occurring during the preparation of Ce<sub>0.9</sub>Gd<sub>0.1</sub>O<sub>2-δ</sub>*



#### *Reactions occurring during the preparation of Ce<sub>0.8</sub>Sm<sub>0.2</sub>O<sub>2-δ</sub>*



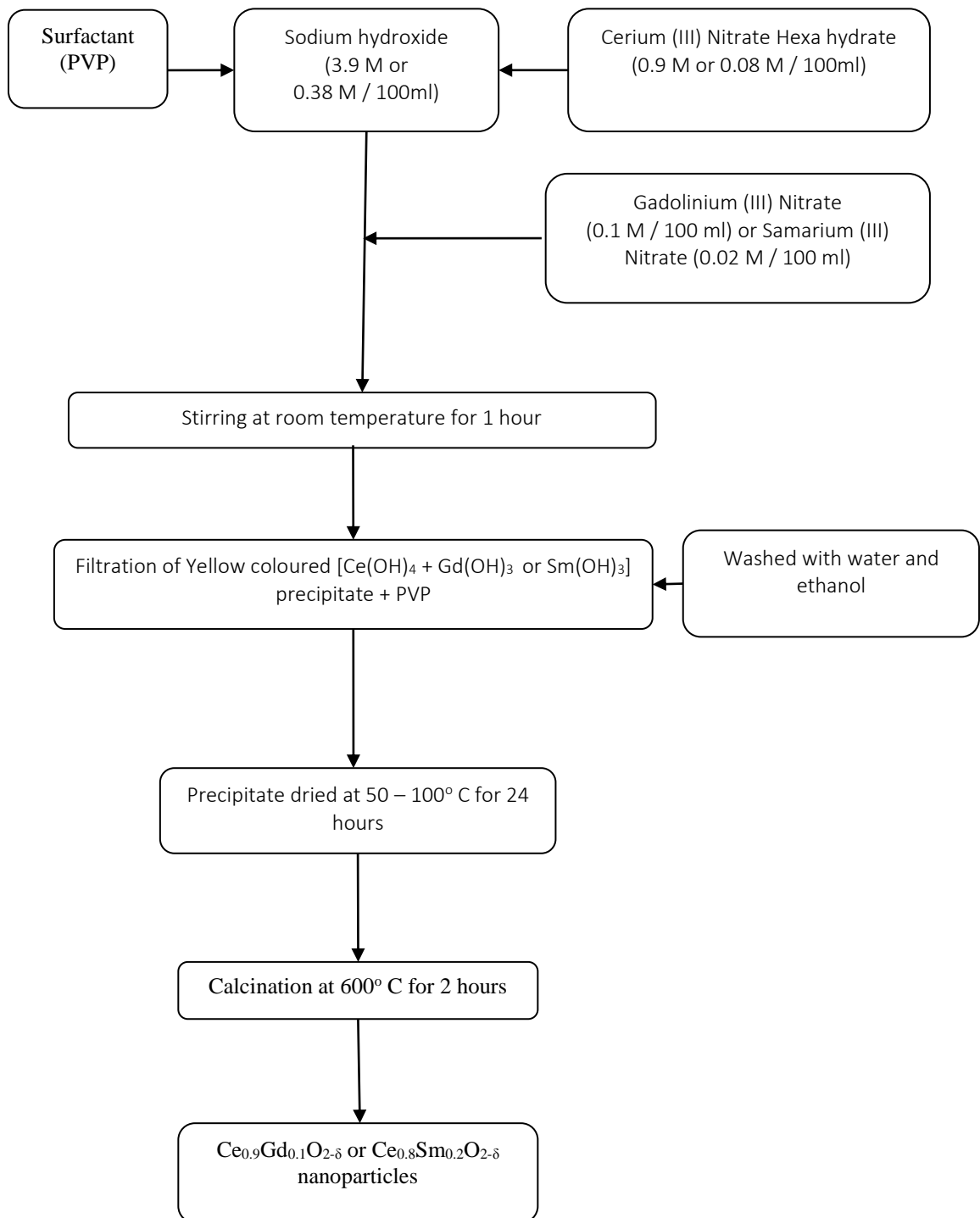


**Figure 1.** Schematic illustration of the synthesis of Ce<sub>0.9</sub>Gd<sub>0.1</sub>O<sub>2-δ</sub> or Ce<sub>0.8</sub>Sm<sub>0.2</sub>O<sub>2-δ</sub> nanoparticles by the chemical precipitation process

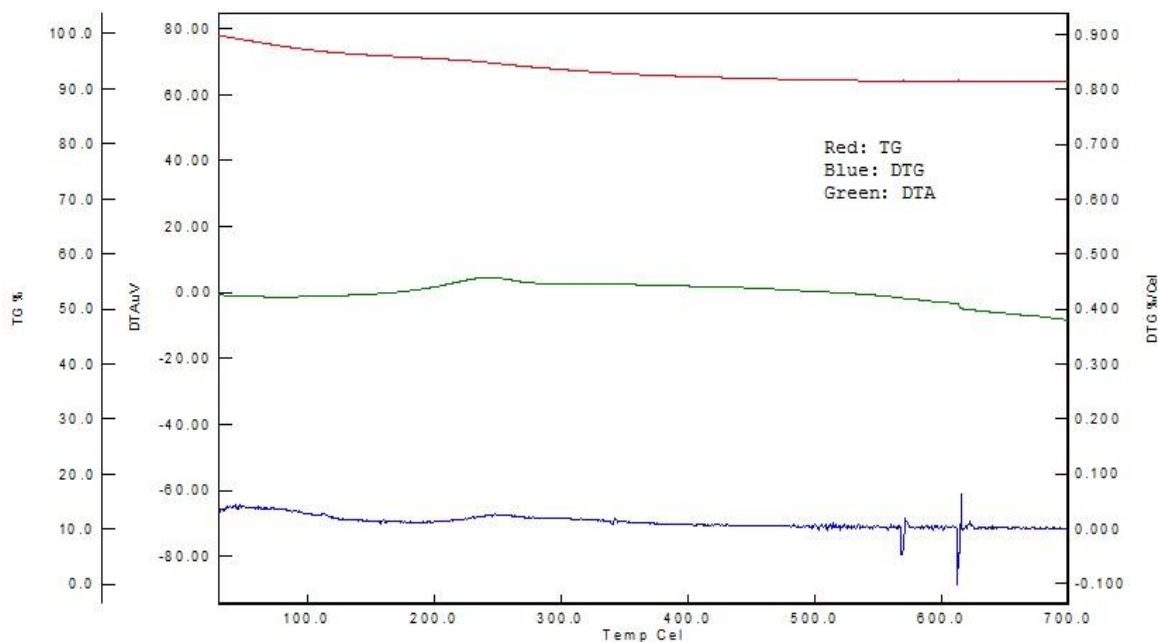


Figure 2. DTA/TGA spectrum obtained on precursor material  $[\text{Ce}(\text{OH})_4 + \text{Gd}(\text{OH})_3 + 2 \text{ ml } 10 \% \text{ PVP}]$

## 2.2. Characterization of the powder

Thermal analysis of the precursor material (mixture of hydroxides) was performed using a SI EXSTAR 6000 TG/DTA 6300 instrument between 25 and 700° C in nitrogen atmosphere. The powder XRD studies were carried out using Shimadzu XRD6000 X-ray diffractometer at a scan speed of 5 deg/min using  $\text{CuK}\alpha$  radiation. The lattice parameters were calculated by least square fitting method using DOS computer programming. The theoretical density of the powders was calculated with the obtained XRD data. The crystallite sizes of the powder were calculated by Scherrer's formula. Bruker IFS 66V FT-IR spectrometer was employed to record the FTIR spectra of doped  $\text{CeO}_2$  powder in the range of 4000 – 400  $\text{cm}^{-1}$ . The particle size of the powder was measured using Malvern Particle Size Analyzer using triple distilled water as medium. The surface morphology of the particles was studied by means of JEOL Model JSM-6360 scanning electron microscope.

## 3. Results and discussion

### 3.1. Thermogravimetry / differential thermal analysis (TGA/DTA) of precursor materials

The TGA/DTA spectrums obtained with the precursor materials  $[(\text{Ce}(\text{OH})_4 + \text{Gd}(\text{OH})_3 + 2 \text{ ml } 10 \% \text{ PVP})$  and  $(\text{Ce}(\text{OH})_4 + \text{Sm}(\text{OH})_3 + 2 \text{ ml } 10 \% \text{ PVP})]$  are indicated in Figures 2 and 3. The DTA peaks closely corresponding to the weight changes observed on the TGA curves. From Figure 2, the total weight loss from the temperature of 25 to 700° C was found to be 9.0%. From the curve, it was understood that the weight loss begins to appear from initial temperature itself. The major weight loss was found between 100 to 230 °C and which may be attributed to the decomposition water molecule and removal of organics from the sample. This was confirmed with an exothermic peak around 230° C. The further weight loss present in the sample until 700° C may be due to the decomposition of oxides of carbon (present in the surfactant) and formation of phase pure doped ceria. From Figure 3, the total weight loss from the temperature of 25 to 500° C was 8.5 %. This reduction in weight was attributed to the removal of water and oxides of carbon present in the sample. From the curve, it was found that the weight loss starts appearing from the initial temperature itself (25° C). The removal of water and other carbon based oxides from the sample may complete at around 240 °C. This was confirmed by an exothermic appeared at 240° C. Around 700° C, the weight loss was found to be stable which indicates the formation of phase pure sample at this temperature.

### 3.2. Structural determination of doped ceria based electrolytes by powder X-ray diffraction

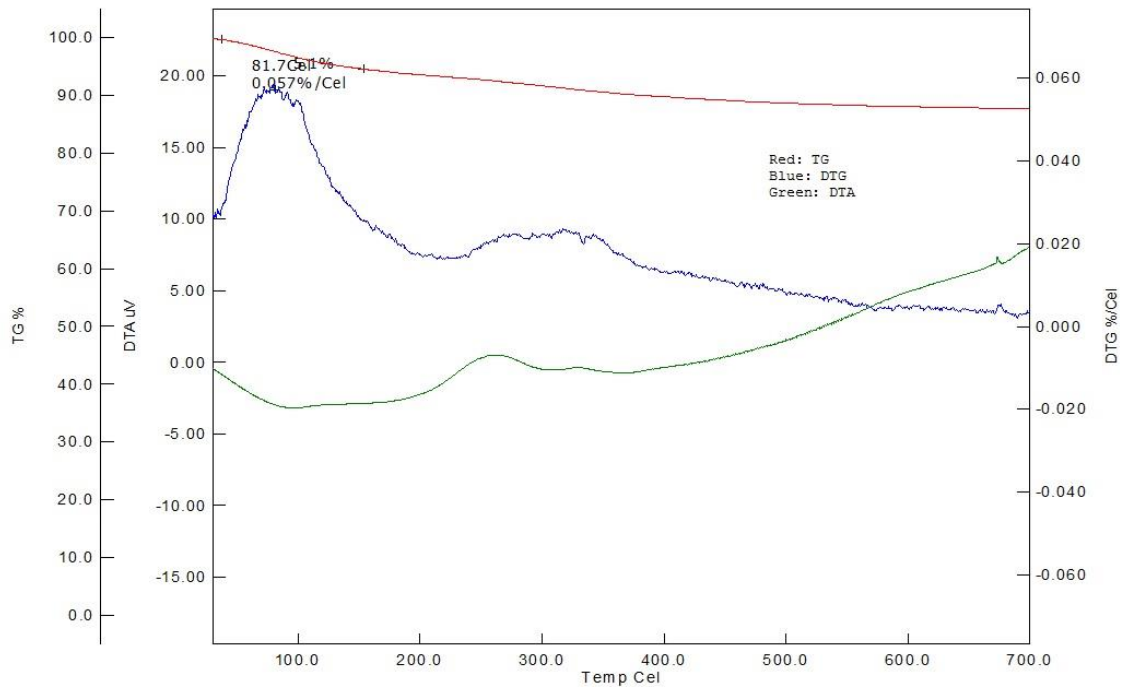


**Figure 3.** DTA/TGA spectrum obtained on precursor material  $[\text{Ce}(\text{OH})_4 + \text{Sm}(\text{OH})_3 + 2 \text{ ml } 10 \% \text{ PVP}]$

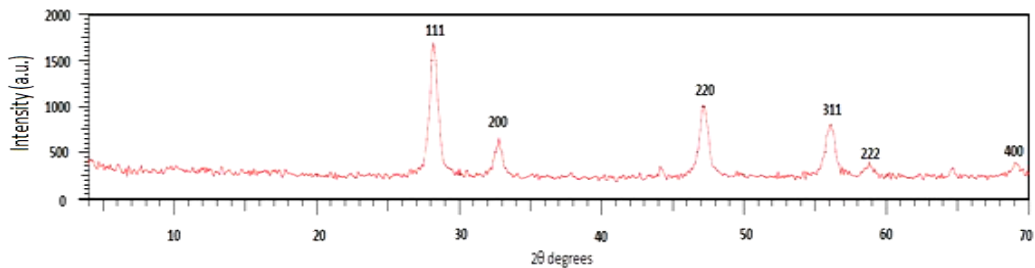


**Figure 4.** XRD pattern obtained on calcined  $\text{Ce}_{0.9}\text{Gd}_{0.1}\text{O}_{2-\delta}$  (CGO) powder prepared by the chemical precipitation method with 2 ml PVP

**Table 1.** XRD data obtained on  $\text{Ce}_{0.9}\text{Gd}_{0.1}\text{O}_{2-\delta}$  (CGO) powder

Standard XRD data for Orthorhombic $\text{CeO}_2$ powder (JCPDS No. 34-0394)			Powder XRD data for $\text{Ce}_{0.9}\text{Gd}_{0.1}\text{O}_{2-\delta}$					
d values (Å)	hkl values	I/I <sub>0</sub>	d <sub>obs</sub> (Å)	d <sub>cal</sub> (Å)	hkl values	2θ values (obs)	2θ values (cal)	I/I <sub>0</sub> (obs)
3.123	111	100	3.163	3.144	111	28.209	28.379	100
2.705	200	30	2.735	2.723	200	32.733	32.885	25
1.913	220	52	1.927	1.925	220	47.161	47.194	55
1.631	311	42	1.642	1.642	311	56.000	55.990	40
1.562	222	8	1.572	1.572	222	58.701	58.717	9
1.353	400	8	1.360	1.361	400	69.017	68.960	11

**Table 2.** Crystal structure and parameters obtained on  $\text{Ce}_{0.9}\text{Gd}_{0.1}\text{O}_{2-\delta}$  (CGO) powder

Properties	Standard XRD data for $\text{CeO}_2$ powder (JCPDS NO. 34-0394)	Obtained XRD data for CGO powder
Crystal structure	Cubic	Cubic
Unit cell lattice parameters ( $\text{\AA}$ )	a = 5.4113	a = 5.4469
Unit cell volume ( $\text{\AA}^3$ )	158.4545	161.6025
Theoretical density (g/cc)	7.2173	7.0734
Crystallite size (nm)	---	9.4529

It has been reported that the XRD patterns of rare earth oxide doped  $\text{CeO}_2$  is similar to that of pure  $\text{CeO}_2$  except slight shifts in diffraction angles [16]. Yahiro et.al found that the system  $\text{Ce}_{1-x}\text{Sm}_x\text{O}_{2-\delta}$  consisted of the solid solution with a fluorite structure at  $x < 50$  at.%. With an increase in  $\text{Sm}_2\text{O}_3$  content, the ionic conductivity decreased due to decrease in mobility of oxygen ions [17]. Torrens et.al have studied by XRD the structural properties of  $\text{Ce}_{0.8}\text{Gd}_{0.2}\text{O}_{2-\delta}$  synthesized through co-precipitation reaction, solid state reaction and hydrothermal synthesis and confirmed that all the powders had single-phase fluorite structure [18]. Yoshida et.al confirmed the structure of samaria doped ceria (SDC) by XRD and it had the fluorite structure [19]. Zhan et.al have observed the X-ray spectra of  $(\text{CeO}_2)_{1-x}(\text{SmO}_{1.5})_x$  ( $0.1 \leq x \leq 0.4$ ) and found that all the samples had a fluorite structure. The lattice parameters of the unit cell of the crystal were shown to increase linearly with the increase in the  $\text{SmO}_{1.5}$  content, indicating full solubility over the investigated range [20].

In this work, the structural properties of  $\text{Ce}_{0.9}\text{Gd}_{0.1}\text{O}_{2-\delta}$  and  $\text{Ce}_{0.8}\text{Sm}_{0.2}\text{O}_{2-\delta}$  synthesized by the chemical precipitation technique are investigated. The as-synthesized powders were yellow in colour. The obtained XRD patterns of doped ceria based electrolyte powders had a cubic (f.c.) fluorite crystal structure. The observed XRD patterns of the doped ceria electrolytes are shown in Figures 4 and 5. All the peaks are very sharp showing the crystalline nature of the heat treated powders. The obtained XRD pattern of the parent  $\text{CeO}_2$  was matched with the standard data for  $\text{CeO}_2$  (JCPDS card No. 34-0394). No other peak corresponding to any impurity is observed in the XRD patterns of the doped ceria based electrolyte powders. The diffraction patterns of the  $\text{Ce}_{0.9}\text{Gd}_{0.1}\text{O}_{2-\delta}$  and  $\text{Ce}_{0.8}\text{Sm}_{0.2}\text{O}_{2-\delta}$  are symmetrical to that of  $\text{CeO}_2$  except for slight shifts in diffraction angles. These shifts are due to dissolution of the additives in the fluorite lattice. The lattice parameters are calculated from  $2\theta$  values in the X-ray diffraction patterns. The powder XRD data obtained on  $\text{Ce}_{0.9}\text{Gd}_{0.1}\text{O}_{2-\delta}$  and  $\text{Ce}_{0.8}\text{Sm}_{0.2}\text{O}_{2-\delta}$  (prepared with 2 ml 10% PVP in the co-precipitation process) are reported in the Tables 1, 2, 3 and 4. The unit cell volumes are also calculated for these oxides. The unit cell volume, crystallite size and theoretical density values are calculated for all the samples and the values were found to be similar to each other. It was reported that the average crystallite size of  $\text{Gd}_2\text{O}_3$  doped  $\text{CeO}_2$  was found to be in the range of 11 nm [21]. The average crystallite size of Gd - doped  $\text{CeO}_2$  by spray pyrolysis was reported as 46 nm [22]. From this, it was understood that our crystallite size values for both the samples are less than the reported data.

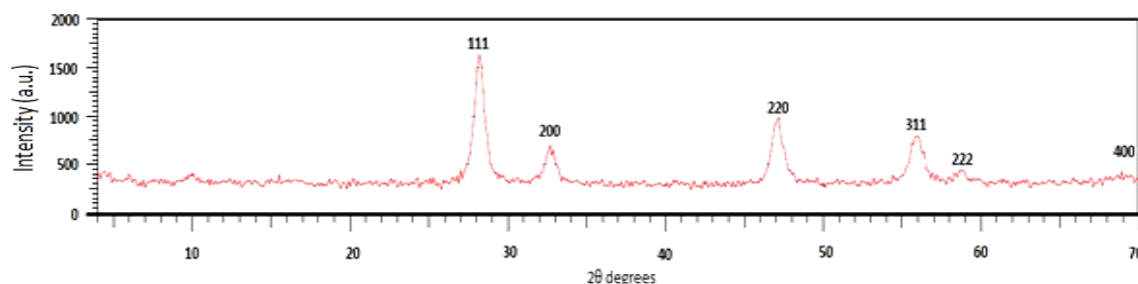


**Figure 5.** XRD pattern obtained on calcined  $\text{Ce}_{0.8}\text{Sm}_{0.2}\text{O}_{2-\delta}$  (CSO) powder prepared by the chemical precipitation method with 2 ml PVP

**Table 3.** XRD data obtained on Ce<sub>0.8</sub>Sm<sub>0.2</sub>O<sub>2-δ</sub> (CSO) powder

Standard XRD data for Orthorhombic CeO <sub>2</sub> powder (JCPDS No. 34-0394)			Powder XRD data for Ce <sub>0.8</sub> Sm <sub>0.2</sub> O <sub>2-δ</sub>					
d values (Å)	hkl values	I/I <sub>o</sub>	d <sub>obs</sub> (Å)	d <sub>cal</sub> (Å)	hkl values	2θ values (obs)	2θ values (cal)	I/I <sub>o</sub> (obs)
3.123	111	100	3.166	3.140	111	28.180	28.415	100
2.705	200	30	2.738	2.720	200	32.696	32.927	28
1.913	220	52	1.931	1.923	220	47.044	47.256	51
1.631	311	42	1.645	1.640	311	55.871	56.066	36
1.562	222	8	1.573	1.570	222	58.673	58.796	10
1.353	400	8	1.354	1.360	400	69.400	69.057	6

**Table 4.** Crystal structure and parameters obtained on Ce<sub>0.8</sub>Sm<sub>0.2</sub>O<sub>2-δ</sub> (CSO) powder

Properties	Standard XRD data for CeO <sub>2</sub> powder (JCPDS NO. 34-0394)	Obtained XRD data for CSO powder
Crystal structure	Cubic	Cubic
Unit cell lattice parameters (Å)	a = 5.4113	a = 5.4402
Unit cell volume (Å <sup>3</sup> )	158.4545	161.0069
Theoretical density (g/cc)	7.2173	7.0996
Crystallite size (nm)	---	8.7138

### 3.3. Fourier transform infrared (FTIR) spectroscopic studies of doped CeO<sub>2</sub> powders

Figures 6 and 7 show the FTIR spectrums obtained on Ce<sub>0.9</sub>Gd<sub>0.1</sub>O<sub>2-δ</sub> (CGO) and Ce<sub>0.8</sub>Sm<sub>0.2</sub>O<sub>2-δ</sub> (CSO) powders prepared by the chemical precipitation method. FTIR measurements were done using KBr method at room temperature (RT). The spectra of both the samples show the absorption band at about 1371 and 1368 cm<sup>-1</sup> respectively which are the characteristic vibration modes of CeO<sub>2</sub> [23]. The samples showed a peak at 2364 and 2363 cm<sup>-1</sup> respectively, are due to the presence of dissolved or atmospheric CO<sub>2</sub> in the sample [24]. The peak appeared at 3280 cm<sup>-1</sup> is related to the O-H stretching vibration of absorbed H<sub>2</sub>O in the CGO sample [25]. This particular peak was absent in case of CSO sample. Rest of the peaks are similar to each other.

**Table 5.** Particle characteristics data (based on intensity) obtained on Ce<sub>0.9</sub>Gd<sub>0.1</sub>O<sub>2-δ</sub> (CGO) powder prepared by chemical precipitation method (with 2 ml PVP)

Trial	Peak 1		Peak 2		Average particle size (d.nm)
	% intensity	Diameter (nm)	% intensity	Diameter (nm)	
Trial - 1	91.2	68.49	8.8	12.02	46.83
Trial - 2	96.9	61.39	3.1	4714	52.34
Trial - 3	100	73.44	--	--	57.20

**Table 6.** Particle characteristics data (based on volume) obtained on Ce<sub>0.9</sub>Gd<sub>0.1</sub>O<sub>2-δ</sub> (CGO) powder prepared by chemical precipitation method (with 2 ml PVP)

Trial	Peak 1		Peak 2		Average particle size (d.nm)
	% volume	Diameter (nm)	%Volume	Diameter(nm)	
Trial - 1	9.4	47.24	90.6	10.64	46.83
Trial - 2	93.6	46.46	6.4	4950	52.34
Trial - 3	100	59.72	--	--	57.20



### 3.4. Particle size measurements obtained on doped CeO<sub>2</sub> powders

The prepared doped ceria particles were subjected to particle size measurements using Malvern particle size analyzer with triple distilled water as medium. For all the measurements, 0.20 g of sample is sonicated in 200 ml triple distilled water for about 5 minutes and after that the sample is subjected for particle size analysis. The particle size distribution curves of the doped samples are shown in Figures 8, 9, 10 and 11.

### 3.5. Particle size distribution data of Ce<sub>0.9</sub>Gd<sub>0.1</sub>O<sub>2-δ</sub> (CGO) powder prepared by chemical precipitation method (with 2 ml PVP)

The particle size distribution curves obtained with CGO powder prepared by chemical precipitation method (with 2 ml PVP) are shown in Figures 8 and 9. The particle characteristics obtained on CGO powder are indicated in Tables 5 and 6. From the Figures 8 and 9 and the particle characteristics data (Tables 5 and 6), it was understood that the average particle size of CGO powder prepared by the chemical precipitation method (with 2 ml PVP) is found to be in the range 46 - 57 nm. The larger particles present in the powder may be due to agglomeration of smaller particles during high temperature treatment.

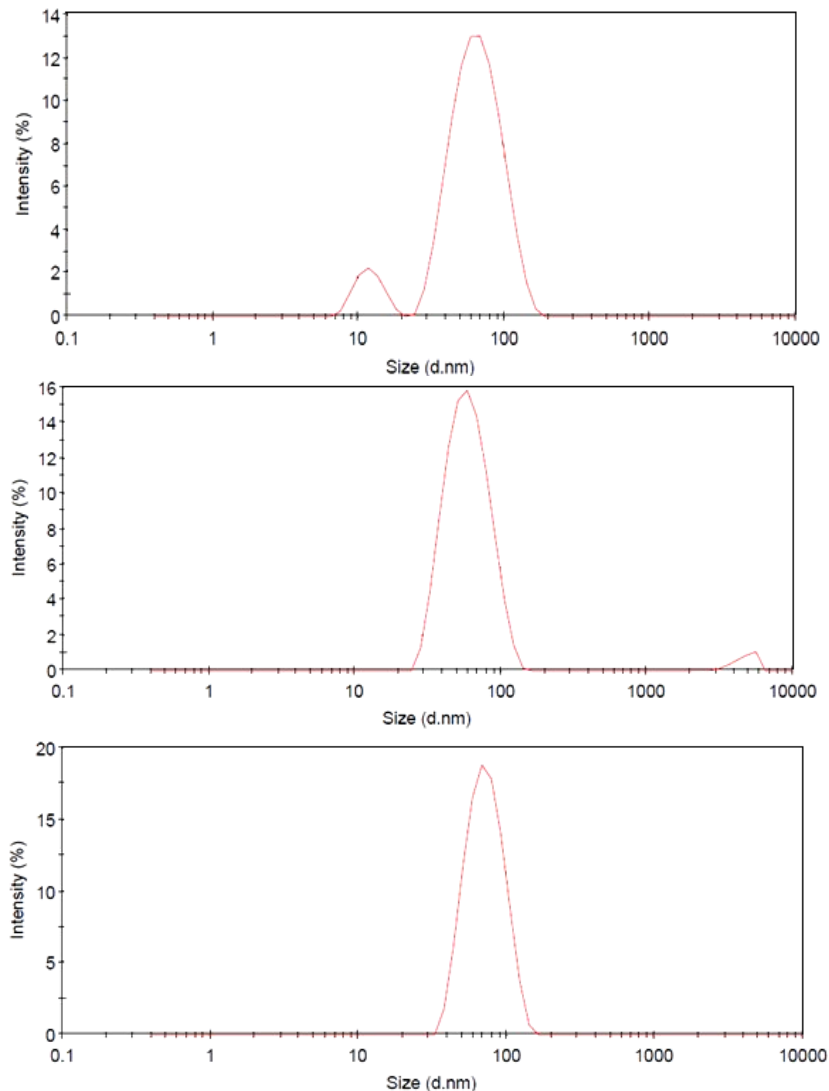


**Figure 8 (a-c).** Particle size distribution patterns (based on intensity) obtained on Ce<sub>0.9</sub>Gd<sub>0.1</sub>O<sub>2-δ</sub> (CGO) powder prepared by the chemical precipitation method (with 2 ml PVP)

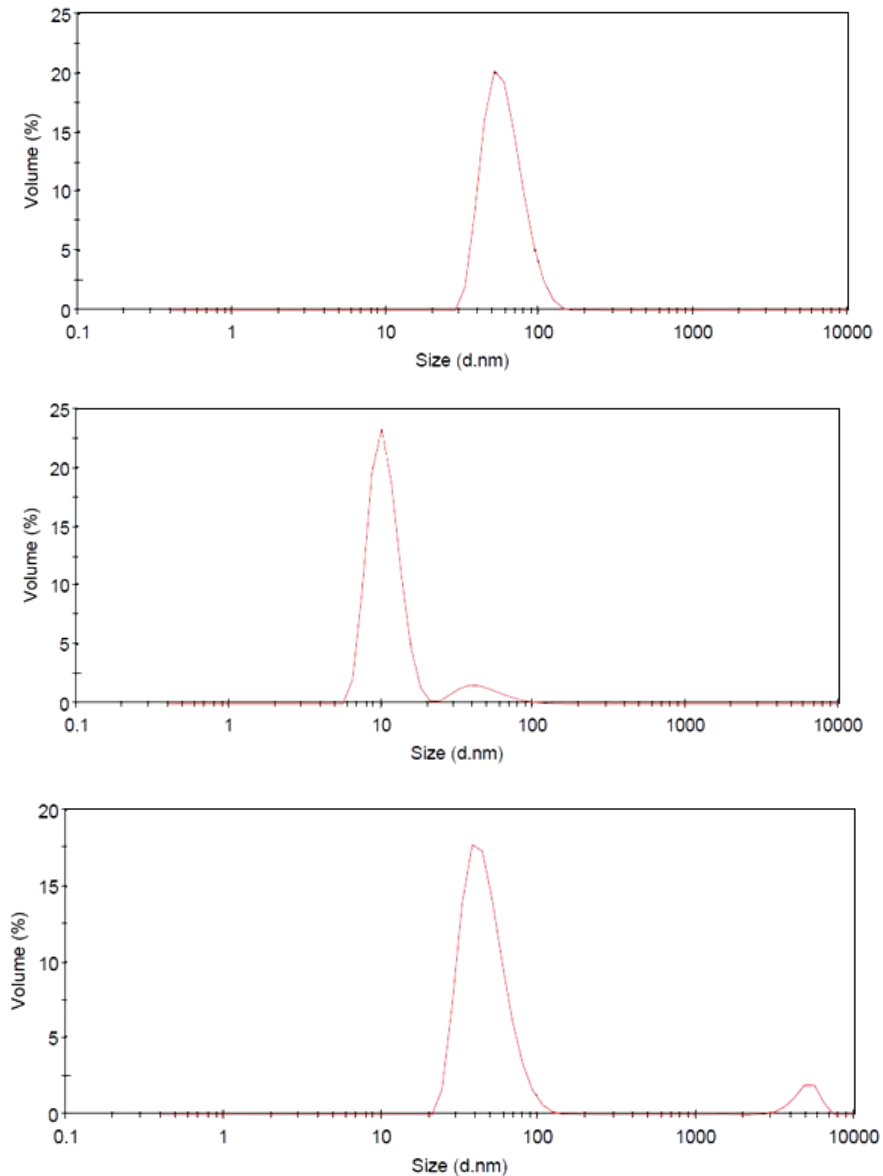


**Figure 9 (a-c).** Particle size distribution patterns (based on volume) obtained on  $\text{Ce}_{0.9}\text{Gd}_{0.1}\text{O}_{2-\delta}$  (CGO) powder prepared by chemical precipitation method (with 2 ml PVP)

### 3.6. Particle size distribution data of $\text{Ce}_{0.8}\text{Sm}_{0.2}\text{O}_{2-\delta}$ (CSO) powder prepared by chemical precipitation method (with 2 ml PVP)

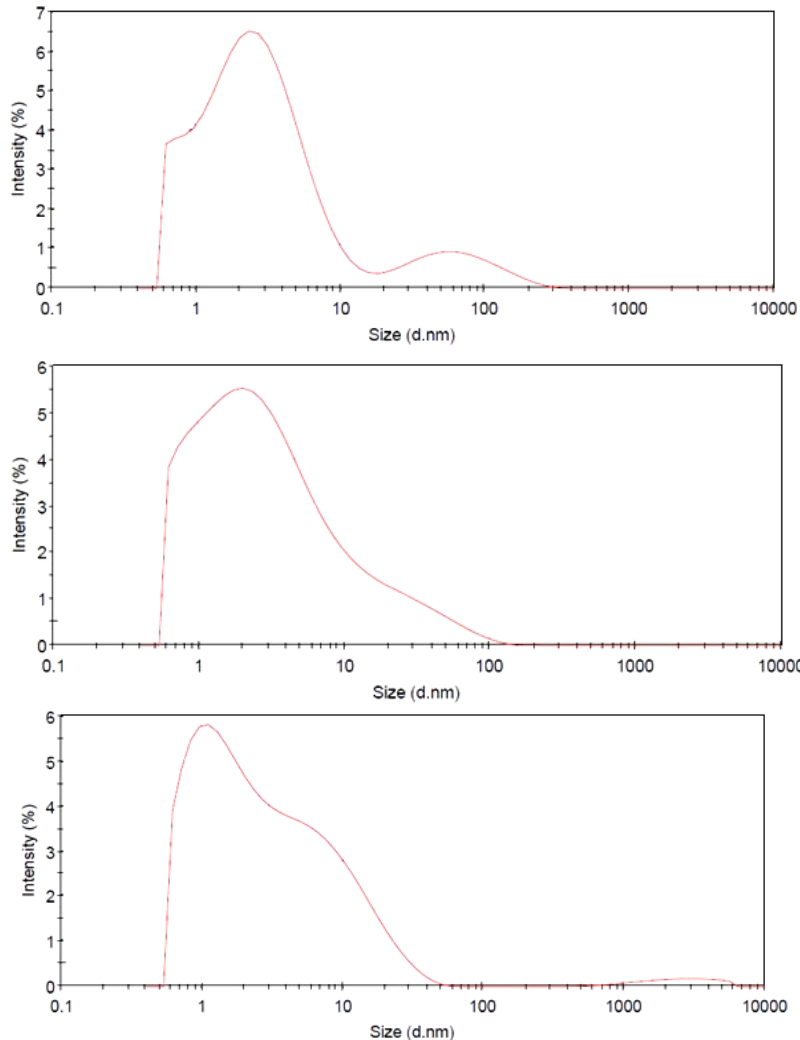
The particle size distribution curves obtained with CSO powder prepared by chemical precipitation method (with 2 ml PVP) are shown in Figures 10 and 11. The particle characteristics obtained on CSO powder are indicated in Tables 7 and 8. From the Figures 10 and 11 and the particle characteristics data (Tables 7 and 8), it was understood that the average particle size of CSO powder prepared by chemical precipitation method (with 2 ml PVP) is found to be in the range 1.796- 1.829 nm, which is very less than the particle size data obtained for CGO sample by the same method of preparation. The presence of the larger particles in the sample may also be to the agglomeration of particles at high temperature treatment.

**Table 7.** Particle characteristics data (based on intensity) obtained on  $Ce_{0.8}Sm_{0.2}O_{2-\delta}$  (CSO) powder prepared by chemical precipitation method (with 2 ml PVP)

Trial	Peak 1		Peak 2		Average particle size (d.nm)
	% intensity	Diameter (nm)	% intensity	Diameter (nm)	
Trial - 1	88.7	3.057	11.3	72.42	1.829
Trial - 2	100	6.691	--	--	1.796
Trial - 3	98	4.805	2	2627	1.796

**Table 8.** Particle characteristics data (based on volume) obtained on  $Ce_{0.8}Sm_{0.2}O_{2-\delta}$  (CSO) powder prepared by chemical precipitation method (with 2 ml PVP)

Trial	Peak 1		Peak 2		Average particle size (d.nm)
	% volume	Diameter (nm)	% volume	Diameter (nm)	
Trial - 1	100	0.9222	--	--	1.829
Trial - 2	100	0.9036	--	--	1.796
Trial - 3	100	0.8911	--	--	1.796

**Figure 10 (a-c).** Particle size distribution patterns (based on intensity) obtained on  $Ce_{0.8}Sm_{0.2}O_{2-\delta}$  (CSO) powder prepared by chemical precipitation method (with 2 ml PVP)

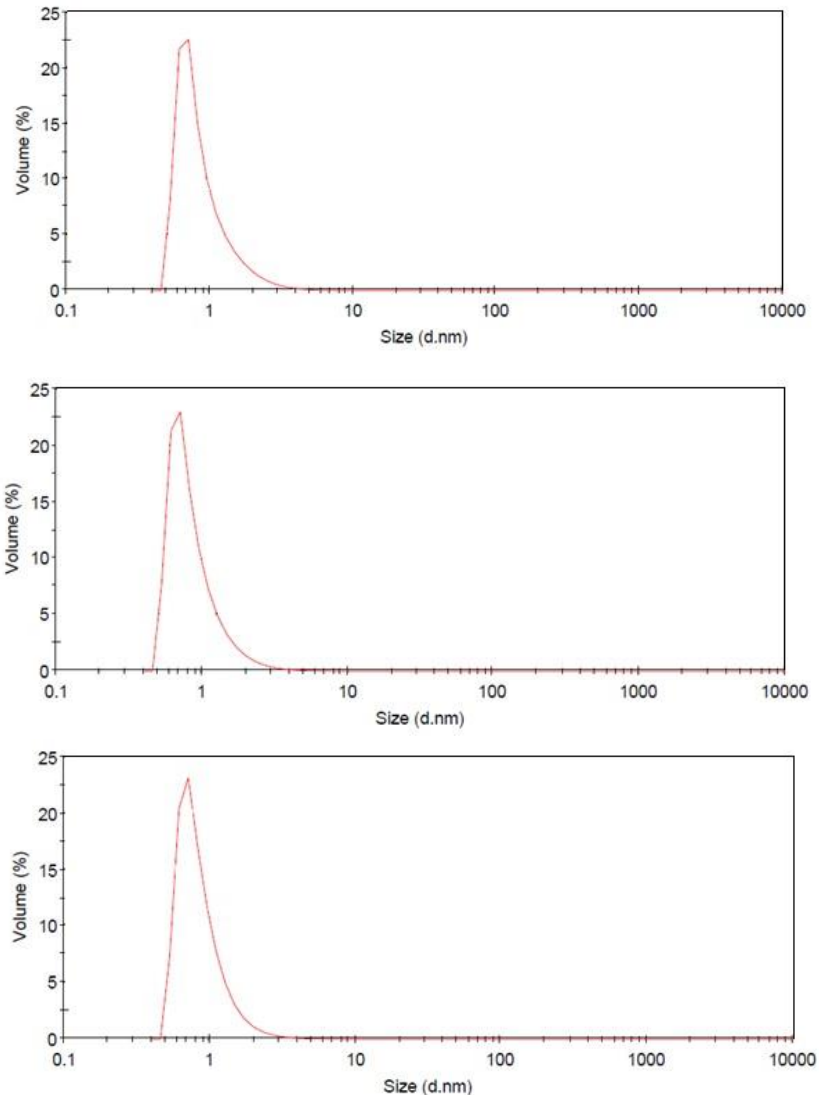


**Figure 11(a-c).** Particle size distribution patterns (based on volume) obtained on  $Ce_{0.8}Sm_{0.2}O_{2-\delta}$  (CSO) powder prepared by chemical precipitation method (with 2 ml PVP)

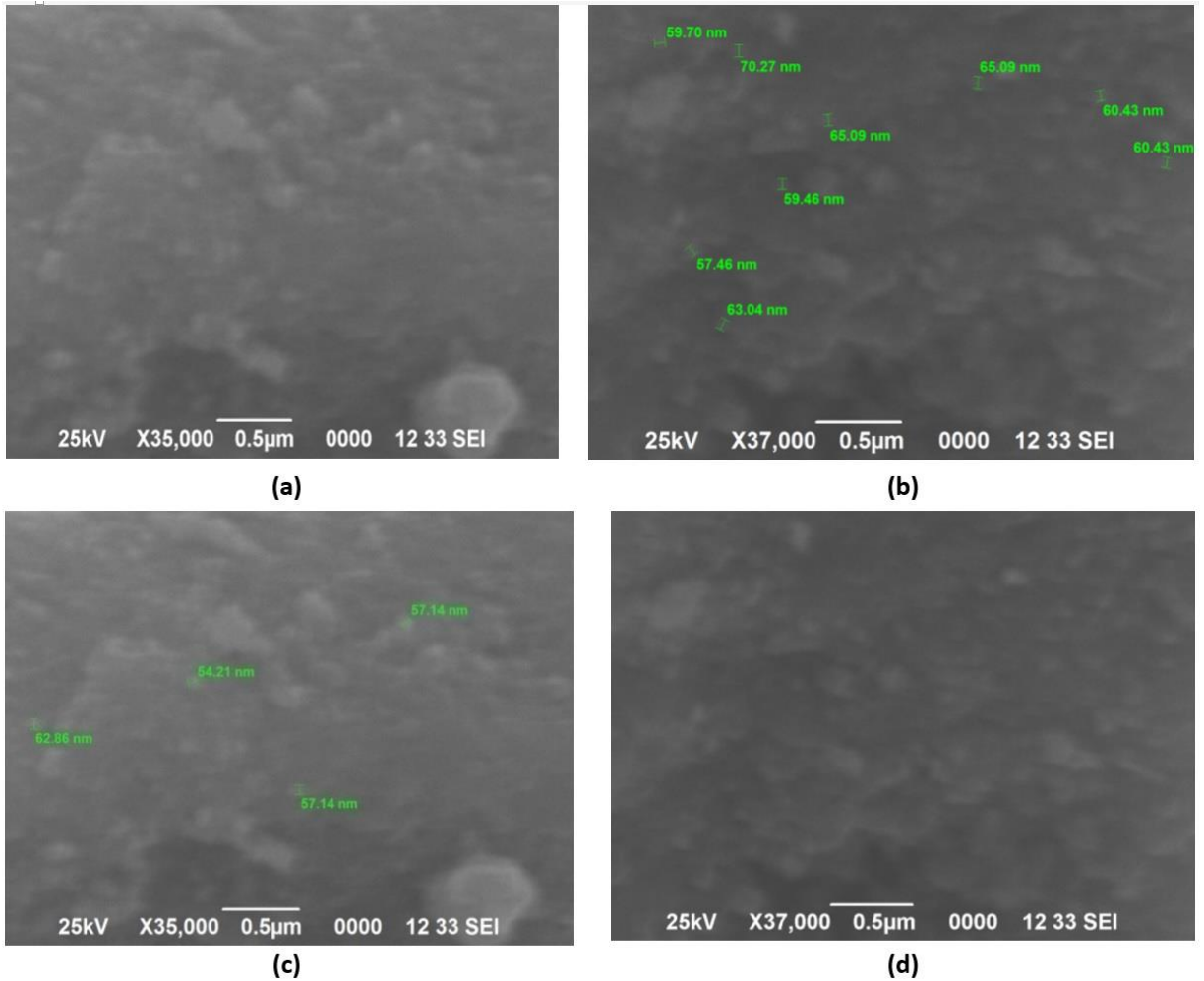
### 3.7 Scanning Electron Microscopic(SEM) studies of doped $CeO_2$ powders

#### $Ce_{0.9}Gd_{0.1}O_{2-\delta}$ (CGO) powder

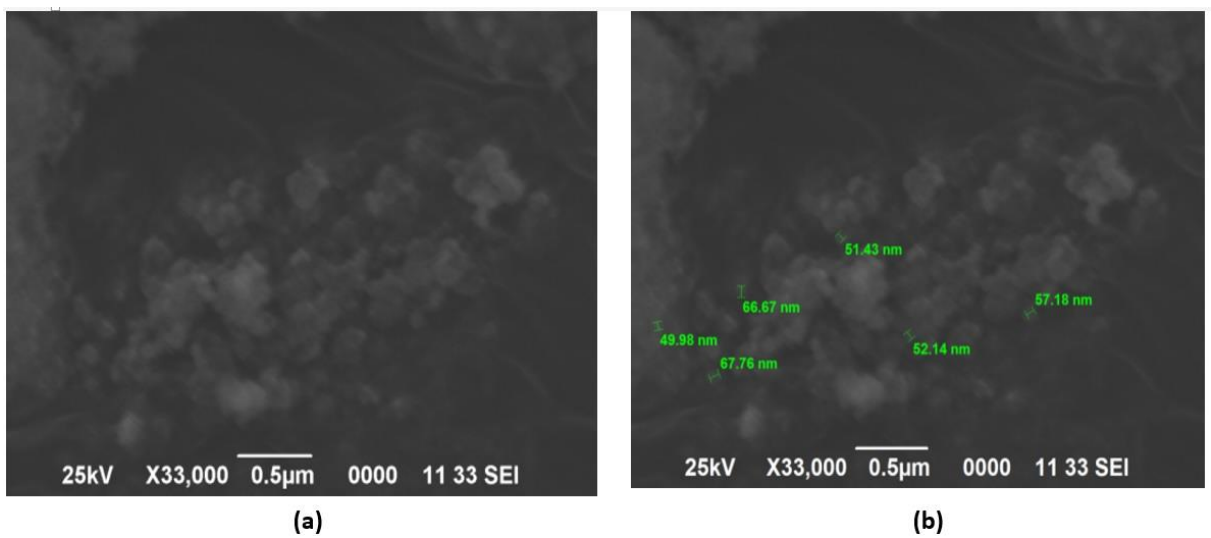
The SEM photographs of the CGO powder prepared by chemical precipitation method with 2 ml PVP as surfactant are indicated in Figure 12. From the micrograph, it was understood that the grains are present in the range of 40 - 50 nm in diameter. Also, the grains were arranged uniformly throughout the structure. The grains were connected with each other and distributed perfectly in the micrograph. In few places, larger grains were also seen. The presence of larger grains may be due to the presence of agglomerated particles in the samples.

#### $Ce_{0.8}Sm_{0.2}O_{2-\delta}$ (CSO) powder

The SEM photographs of the CSO powder prepared by chemical precipitation method with 2 ml PVP as surfactant are indicated in Figure 13. In this micrograph, different variety (in diameter) of grains were present. The grains were present together. The grain size is varied from 25 to 50 nm. From the particle characteristics and SEM data, it was confirmed that the samples have nanoparticles in them.



**Figure 12 (a-d).** SEM Photographs obtained on calcined  $\text{Ce}_{0.9}\text{Gd}_{0.1}\text{O}_{2-\delta}$  (CGO) powder prepared by the chemical precipitation with 2 ml PVP



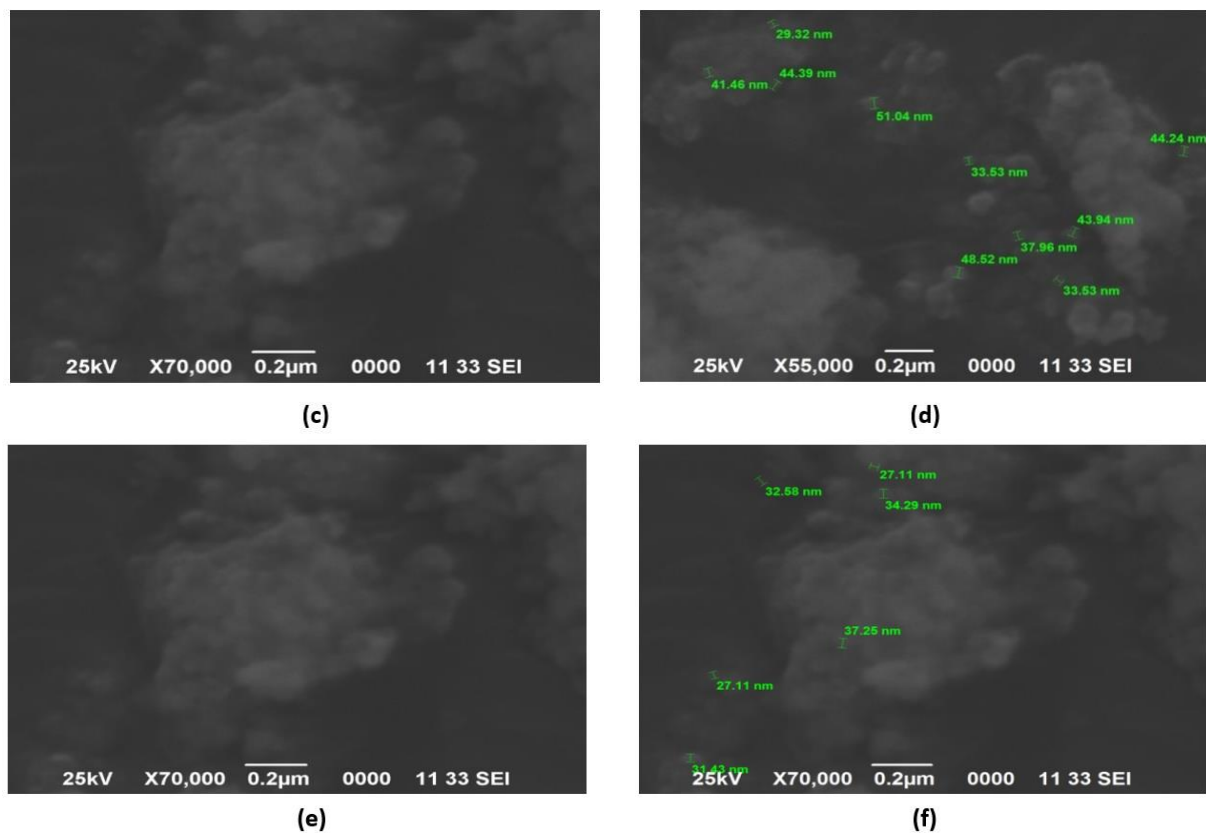


**Figure 13 (a-f).** SEM Photographs obtained on calcined  $\text{Ce}_{0.8}\text{Sm}_{0.2}\text{O}_{2-\delta}$  (CSO) powder prepared by the chemical precipitation with 2 ml PVP

#### 4. Conclusion

Chemical precipitation process can be effectively used for the preparation of  $\text{Ce}_{0.9}\text{Gd}_{0.1}\text{O}_{2-\delta}$  (CGO) and  $\text{Ce}_{0.8}\text{Sm}_{0.2}\text{O}_{2-\delta}$  (CSO) nanoparticles which might be used as alternate electrolyte materials for low temperature solid oxide fuel cells (LTSOFCs). The TGA/ DTA studies gave an idea about the decomposition of products from the precursor materials. The powder XRD data obtained on doped powder is in good agreement with the standard reported data. From the FTIR data, it is derived that all samples exhibited characteristic peak for  $\text{CeO}_2$ . The particulate properties obtained on  $\text{CeO}_2$  powder confirmed the presence of nano particles in the samples. The existence of uniform sized with grain size of 50 – 100 nm was proved by SEM.

#### 5. Acknowledgement

ASN thanks Karunya University for promoting high temperature fuel cell research activity in the University. He thanks Dr. P. E. Jagadeesh Babu, NITK, Surathkal, India for his help in TG-DTA measurements.

#### References

- [1] B. C. H. Steele, Solid State Ionics, 129, 95 (2000).
- [2] H. Inaba and H. Tagawa, Solid State Ionics, 83, 1 (1996).
- [3] J. Luo, R.J. Ball and R. Stevens, J. Mater Science, 39, 235 (2004).
- [4] T. Kudo and Y. Obayashi, J. Electrochem. Soc., 123, 415 (1976).
- [5] B.C.H. Steele, In Proceedings of the 1<sup>st</sup> European SOFC Forum, Lucerne, Switzerland pp.375-397 (1994).

- [6] Rajiv Doshi, Von L. Richards, J. D. Carter, Xiaoping Wang and Michael Krumpelt, *J. Electrochem. Soc.*, 146, 1273 (1999).
- [7] J.P.P. Huijsmans, F.P.F. van Berkel and G.M. Christie, *J. Power Sources*, 71, 107 (1998).
- [8] C. Milliken, S. Guruswamy and A. Khandkar, *J. Electrochem. Soc.*, 146, 872 (1999).
- [9] Stephanie J.A. Livermore, John W. Cotton and R. Mark Ormerod, *J. Power Sources*, 86, 411 (2000).
- [10] V. V. Kharton, F. M. Figueiredo, L. Navarro, E. N. Naumovich, A. V. Kovalevsky, A. A. Yaremchenko, A. P. Viskup, A. Carneiro, F. M. B. Marques and J. R. Frade, *J. Mater. Science*, 36, 1105 (2001).
- [11] Toshiyuki Mori, Richard Buchanan, Ding Rong Ou, Fei Ye, Tomoaki Kobayashi, Je-Deok Kim, Jin Zou and John Drennan, *J. Solid State Electrochem.*, 12, 841 (2008).
- [12] H. Yahiro, Y. Eguchi, K. Eguchi and H. Arai, *J. Appl. Electrochem.*, 18, 527 (1988).
- [13] B.C. H. Steele, "High conductivity solid ionic conductors, recent trends and applications", ed. T. Takahashi, 1989, World Scientific, London, 402.
- [14] Z. Tianshu, P. Hing, H. Huang and J. Kilner, *Solid State Ionics*, 148, 567 (2002).
- [15] Quan Yuan, Hao-Hong Duan, Le-Le Li, Ling-Dong Sun, Ya-Wen Zhang and Chun-Hua Yan, *J. Colloid and Interface Science*, 335, 151 (2009).
- [16] Feng-Yun Wang, Ben-Zu Wan and Soofin Cheng, *J. Solid State Electrochem.*, 9, 168 (2005).
- [17] Hidenori Yahiro, Koichi Eguchi and Hiromichi Arai, *Solid State Ionics*, 21, 37 (1986).
- [18] R.S. Torrens, N.M. Sammes and G.A. Tompsett, *Solid State Ionics*, 111, 9 (1998).
- [19] Hiroyuki Yoshida, Kazuhiro Miura, Jun-ichi Fujita and Toru Inagaki, *J. Am. Ceram. Soc.*, 82, 219 (2004).
- [20] Zhongliang Zhan, Ting-Lian Wen, Hengyong Tu and Zhi-Yi Lu, *J. Electrochem. Soc.*, 148, A 427 (2001).
- [21] Oleg Vasykiv and Yoshio Sakka, *Nano Lett.*, 5, 2568 (2005).
- [22] Hee Song Kang, Jong Rak Sohn, Yun Chankang, Kyeong Youl Jung and Seung Bin Park, *J. Alloys and Compounds*, 398, 240 (2005).
- [23] B. Yan and H. Zhu, *J. Nanoparticle Res.*, 10, 1279 (2008).
- [24] A. C. Tas, P. J. Majewski and F. Aldinger, *J. Am. Ceram. Soc.*, 83, 2954 (2000).
- A.A. Ansari and A. Kaushik, *J. Semiconductors*, 31, 033001-1 (2010).